
Since January 2020 Elsevier has created a COVID-19 resource centre with free information in English and Mandarin on the novel coronavirus COVID-19. The COVID-19 resource centre is hosted on Elsevier Connect, the company's public news and information website.

Elsevier hereby grants permission to make all its COVID-19-related research that is available on the COVID-19 resource centre - including this research content - immediately available in PubMed Central and other publicly funded repositories, such as the WHO COVID database with rights for unrestricted research re-use and analyses in any form or by any means with acknowledgement of the original source. These permissions are granted for free by Elsevier for as long as the COVID-19 resource centre remains active.

Tetrahedron 68 (2012) 4346–4352

Contents lists available at SciVerse ScienceDirect

Tetrahedron

journal homepage: www.elsevier.com/locate/tet

# A multivalent HIV-1 fusion inhibitor based on small helical foldamers

Cristian Guarise [a], Sandip Shinde [b], Karen Kibler [c], Giovanna Ghirlanda [b], Leonard J. Prins [a], Paolo Scrimin [a,*]

[a] University of Padova, Department of Chemical Sciences, via Marzolo 1, 35131 Padova, Italy
[b] Arizona State University, Department of Chemistry and Biochemistry, PO Box 871604, Tempe, AZ 85287-1604, USA
[c] The Biodesign Institute at the Arizona State University, Center for Infectious Diseases and Vaccinology, Tempe, AZ 85287-5401, USA

ARTICLE INFO

*Article history:*
Received 14 November 2011
Received in revised form 21 February 2012
Accepted 20 March 2012
Available online 7 April 2012

*Keywords:*
Peptide foldamer
α-Aminoisobutyric acid
HIV-1 inhibition
Peptide template
$3_{10}$-Helix

ABSTRACT

The peptide sequence AcNH–TEG–Glu-Aib-Trp-AibAib-Trp-AibAib-Ile-Asp–OH (**1**), designed to display the WWI epitope found near the C-terminus of gp41, an envelope glycoprotein decorating the surface of the HIV-1 virus, has been synthesized and proved to have a relevant content of helical conformation because of the presence of five α-aminoisobutyric acid (Aib) units. Three copies of it have been connected to a tripodal platform based on 2,4,6-triethylbenzene-1,3,5-trimethylamine. The tripodal template **2** is even more structured than **1** thus suggesting a significant interaction between the three sequences connected to the platform. Preliminary inhibition assays of HIV-mediated cell fusion indicated that while the single peptide **1** is inactive within the concentration range of our assay, when it is conjugated to the tripodal platform, it is moderately active. These promising results suggest that our approach constitute a valid alternative to those reported so far.

© 2012 Elsevier Ltd. All rights reserved.

## 1. Introduction

HIV-1 entry into target cells is a multistep process involving a series of viral proteins and host-cell receptors. The envelope glycoprotein assembly formed by gp120 and gp41, which decorate the surface of HIV-1, plays key roles in this process.[1–4] Gp120 engages CD4 and CCR5 or CXCR4 co-receptors primarily on macrophages and $CD4^+$ T cells and subsequently undergoes a conformational change, which activates (basically uncloaks) gp41. The ectodomain (extraviral) of gp41 consists of three important regions: an N-terminal fusion sequence that inserts into the target cell membrane, and two helical regions containing two hydrophobic heptad repeat units (denoted as the N- and C-helical regions, respectively). The N-HR regions of three gp41 molecules form a trimeric α-helical coiled-coil. Upon dissociation of gp120 from the complex, a six-helix bundle forms in which the C-helical regions wrap around the inner coil in an antiparallel fashion (trimer-of-hairpins, Fig. 1). The formation of the six-helix bundle is essential for the complete fusion of the virus and target cell membranes.[5] Notably, this mechanism of virus entry has also been observed in Ebola virus, Newcastle disease virus, respiratory syncytial virus and the corona virus. In all these cases the fusion glycoprotein forms a rod-shaped α-helical bundle.[6]

Fusion inhibitors are a highly attractive therapeutic concept since they block HIV-1 at the very first action level, that is, before cell entry.[7–9]

This is in contrast with the more frequently used nucleoside/nucleotide inhibitors of reverse transcriptase or the protease

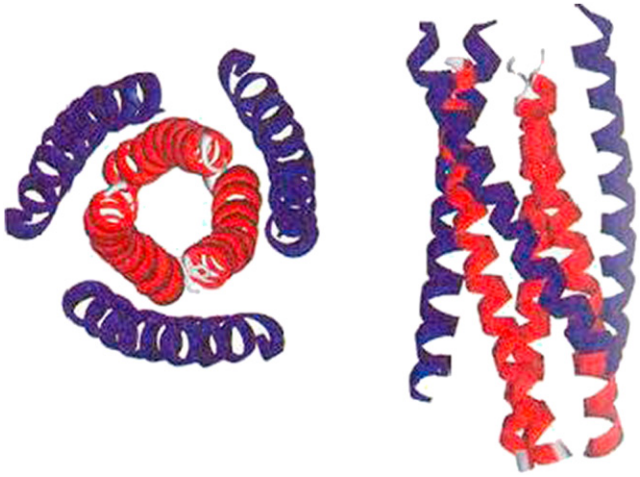

**Fig. 1.** Top and side views of the crystal structure of the fusion active six-helix bundle. The helices correspond to the N36 (red) and the C34 (blue) helical regions.[5b]

* Corresponding author. Tel.: +39 (0)49 8275276; e-mail address: paolo.scrimin@unipd.it (P. Scrimin).

0040-4020/$ – see front matter © 2012 Elsevier Ltd. All rights reserved.
doi:10.1016/j.tet.2012.03.078

inhibitors.[10] Further, the analogy of the HIV-1 fusion mechanism with other viruses suggests a very wide scope for this kind of therapeutic agents.[11,12] T-20 (also termed DP178, enfuvirtide and marketed as Fuzeon by Roche) is a peptide that comprises the C-terminal 36 amino acids of the C-helical domain and strongly inhibits HIV-1 replication by binding to the inner trimeric coiled coil, thus preventing the formation of the six-helix bundle.[13] Unfortunately widespread use of the molecule is plagued by several disadvantages: a difficult and expensive synthesis, inactivation by gut peptidases that prevent oral administration and intestinal absorption in an active form, and a short terminal elimination half-life (less than 4 h) that makes subcutaneous drug delivery necessary (90 mg, twice daily). Consequently, there is an extensive search for small (peptide-like) molecules that have the same mechanistic effect as T-20, but with improved pharmacological properties. Over the years, small simple[14,15] and constrained[16–18] α-peptides, β-peptide,[19] α–β peptides,[20] aromatic foldamers,[21] D-peptides derived from phage display,[22] and peptide-small molecule conjugates[23] have been proposed. Generally, these inhibitors target only a hydrophobic pocket in the α-helical coiled-coil, which in the native protein is occupied by three α-helical residues found near the gp41 C-terminus: Trp628, Trp631, and Ile635 (the WWI epitope).[24–26] Schepartz et al. prepared a series of $\beta^3$-decapeptides in which the WWI epitope is presented on one face of a short 14-helix.[19] It was shown that these β-peptides bind to a gp41 model in vitro and inhibit gp41-mediated fusion in cell culture. Activities were similar to other small molecules reported before ($IC_{50}$ values between 5 and 26 μM, respectively), but much less potent than Fuzeon (which has an $IC_{50}$ value of 0.11 nM).[27] However, compared to Fuzeon these $\beta^3$-decapeptides have the advantage of being one-third the size, having higher metabolical stability and being amenable to (combinatorial) optimization.

Although appealing, the β-peptide foldamers (or better the 14-helix) may not present the optimal scaffold for expressing the WWI epitope, because of the relatively large difference between the 14- and the native α-helix.[28] Rather, an attractive alternative may be the expression of the WWI epitope on a small $3_{10}$-helix, which bears much closer resemblance to the α-helix. The $3_{10}$-helix is induced in small oligopeptides (down to 7–8 residues) when more than 4–5 α-aminoisobutyric acid (Aib) residues are present, exposing amino acids in $i$ and $i+3$ positions on the same face of the helix.[29–34] Like the β-peptides, $C^{\alpha}$-tetrasubstituted amino acids increase the metabolic stability of the resulting peptides. Previously, Sia et al. have reported on the inhibition of HIV-1 entry using short peptides (14 residues) that were conformationally constrained either by using covalent linkers or Aib.[17] Based on these studies they concluded that no correlation exists between the inhibitory potency and the helical content of the oligopeptides. However, it should be noted that none of the peptides showed any helicity at all when free in solution. This can be explained by the small number of Aibs present (2) and the rather arbitrary sites of covalent side-chain linkers. The trimeric α-helical coiled coil forms an interesting target also from the perspective of multivalency, which relates directly to current interests in our group. The $C_3$-symmetry of the α-helical bundle implies that three identical binding sites for the WWI epitope are present. Template constructs have been used to stabilize the N-terminal peptide of gp41, with the purpose of inducing immunological reactions or simply as stable target for the development of fusion inhibitors.[35,36] Conversely, a significant gain in binding affinity may be observed when multiple copies of the inhibitory peptide are connected to a scaffold molecule (with appropriate flexible spacers that can span the required distance). Following this approach, three copies of T-20 were ligated to a scaffold molecule by Tam and Yu.[30] Preliminary results showed a modest 10-fold increase in inhibitory potency with respect to the monomeric peptide, which may be related to the rather small linkers used to connect the three copies together. In contrast, dimerization and trimerization of non helical D-peptide binders of gp41 selected by phage display resulted in increased antiviral activity by 300- and 2500-fold, respectively, over the monomeric version (PIE7).[22b] Alternatively, Wang and co-workers used a monosaccharide as scaffold to link up to four copies of T-20 in order to be used as an immunogen for raising high-titer antibodies against HIV-1.[38] From a more fundamental point of view, it would be interesting to determine the interactions between three $3_{10}$-helices connected to a scaffold, which potentially may lead to superstructures such as a trimeric coiled coil.[39,40]

Based on these premises we planned to prepare a short (10 residues) peptide rich in the tetrasubstituted amino acid Aib, able to induce an helical conformation, designed to display the WWI epitope and connect it to a tripodal platform based on a 2,4,6-triethylbenzene-1,3,5-trimethylamine (Fig. 2). It is well documented that the three substituents on alternating position of a hexasubstituted benzene point toward the same direction, either above or below the benzene-plane.

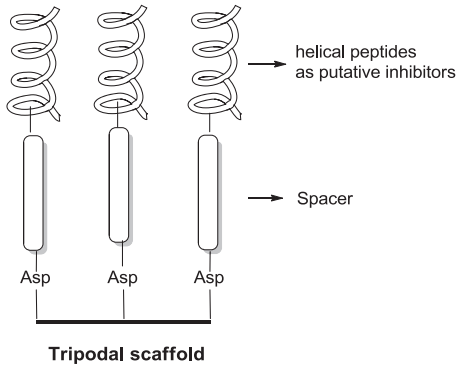


**Fig. 2.** Design of the multivalent HIV-1 fusion inhibitors based on small helical foldamers connected to a tripodal scaffold.

To determine whether α-helix or $3_{10}$-helix is better suited to display the WWI, we modeled both structures using pertinent canonical $\varphi$ and $\psi$ torsion angles The top view (Fig. 3) shows a significant discrepancy in the position of the I-residue. Removing one residue between Trp (W) and Ile (I), neatly aligns the three relevant residues forming a hydrophopic flank.

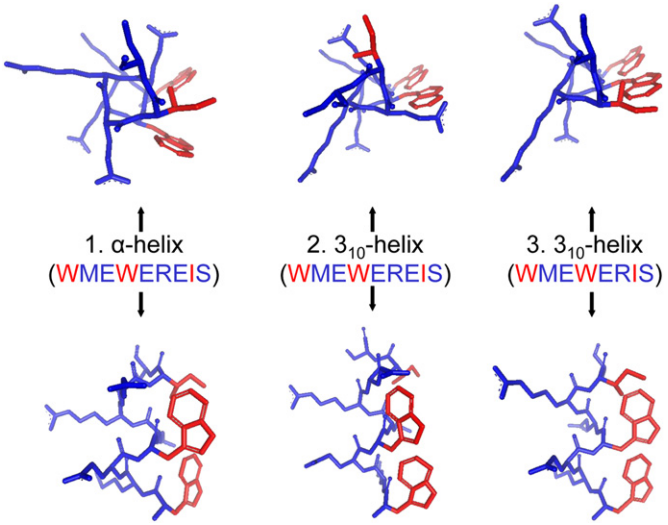


**Fig. 3.** The relevant sequence imposed on an α-helix (1), a $3_{10}$-helix (2) and the same sequence in which one residue between W (Trp) and I (Ile) is eliminated imposed on a $3_{10}$-helix (3). WWI-residues in red. Helical conformations are reported with canonical torsion angles.

## 2. Results and discussion

### 2.1. Synthesis of the peptides

We selected the following core sequence as target peptide: $H_2N$–*Trp*AibAib*Trp*AibAib*Ile*–COOH. We did not anticipate significant difficulties in the synthesis, as the Aib residues can be introduced as dimers on solid support following a recently published procedure.[41] However, this sequence is extremely apolar and we predicted that it would not be soluble in polar media. To increase the solubility of the peptide, we have added Glu and Asp residues at the N- and C-termini, respectively, and a triethylene glycol (TEG) spacer at the N terminus. Accordingly we focused on the following sequence:

AcNH–TEG–Glu-Aib-*Trp*-AibAib-*Trp*-AibAib-*Ile*-Asp–OH (**1**)

Peptide **1** was synthesized on Wang resin (by solid phase peptide synthesis, SPPS) following standard Fmoc chemistry. To avoid the known problems related to the consecutive coupling of Aib residues during SPPS, the dimer Fmoc–Aib-Aib–OH, to be introduced as such, has been prepared in solution in good yields (Fig. 4).

The synthesis of **1** was carried out following three different protocols: the first one by using conventional heating under standard SPPS conditions gave unacceptable low purity of the product (see Fig. S1 of Supplementary data) while the second one, under microwave (MW) irradiation (5 min, 59 W, 75 °C) gave a 50% purity of the crude (see Fig. S1 of Supplementary data). This is in accord with recent findings reporting MW as a valuable alternative in SPPS synthesis when hindered amino acids are used.[42] After purification it was immediately apparent that, although peptide **1** was the major product of the crude, the overall yield was unacceptably low (ca. 5%). This is likely due to the fact that the Wang resin is not particularly stable under MW irradiation. Indeed we have observed (data not reported) that the PAL resin, a polyethylene glycol-based resin with a very high degree of cross-linking, is much more compatible with MW irradiation (yield increased to ca. 35%).

However, when the same synthesis was repeated without MW irradiation, following standard Fmoc chemistry but adding each single amino acid previously activated with cyanuric fluoride much better results were obtained. The coupling with Fmoc–Aib-Aib–F failed (an intramolecular cyclization was likely occurring), while the use of Fmoc–Aib–F gave an impressive 90% yield.

### 2.2. Synthesis of the tripodal peptide template

Having successfully synthesized peptide **1**, we then planned, as the most obvious strategy, to connect three copies of it to the scaffold 1,3,5-tris-(aminomethyl)-2,4,6-triethylbenzene using our previously reported methodology for the functionalization of scaffold molecules on solid support, which does not require (partial) protection of the scaffold or a special functional group arrangement on it, while maintaining scaffold symmetry in the final product.[43] In this way it is possible to obtain the scaffold, functionalized with three aspartic acid residues, linked to Wang resin. After removal of the protecting groups the scaffold has three amino groups at the ends, which can be reacted with an Fmoc–PEG spacer (20)–OH and, subsequently, to the peptide taking advantage of the presence of the carboxylate in the Cα of Asp at the C terminus. For this purpose the allyl-protected peptide **1a** (AcNH–TEG–Glu(All)-Aib-*Trp*-AibAib-*Trp*-AibAib-*Ile*-Asp(OH)–OAll) was synthesized using Fmoc–Glu(All)–OH and Fmoc–Asp(OH)–OAll. After the coupling reaction, the allyl can be easily be removed with Pd(0)–Tetrakis catalyst and $PhSiH_3$ before the cleavage. Obviously, as an alternative approach, the final tripodal peptide template can be obtained with the sequential coupling of the single amino acids. The successful strategy is shown in Fig. 5.

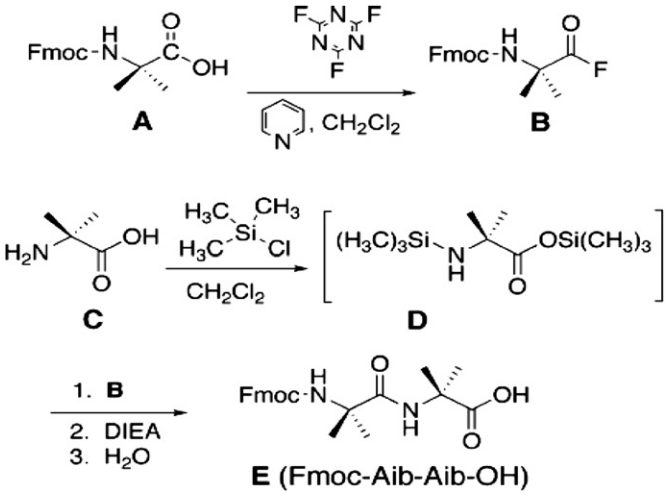


**Fig. 4.** Protocol followed for the solution synthesis of Fmoc–Aib-Aib–OH.

By operating under standard coupling conditions (35 °C, 12 h) and a two-fold excess of **1a**, HPLC–MS of the crude reaction product after removal from the resin showed the formation of the mono-adduct as the most abundant product, followed by the di-adduct and very little amount of the desired tri-adduct. Because of the unavailability of a large excess of peptide **1a** it became immediately clear that this strategy could not be pursued with success. Accordingly we followed the step by step elongation of the peptide in the three arms of the platform. In this regard the activation of the carboxylic acid as the fluoride and of the amino group with *N*,*O*-bis(trymethylsilyl)acetamide (BSA) proved indispensable for achieving high yields in the coupling reactions.[44] By using this strategy the expected tripodal product was obtained in a ca. 10% overall yield even without using MW irradiation. The HPLC trace of **2** and its MS spectrum are reported in Fig. 6.

### 2.3. Conformational studies on peptide 1 and the tripodal peptide template 2

In order to assess the conformational stability of the peptides synthesized and of the tripodal template based on peptide **1** we have run CD spectra in different solvents. They are reported in Fig. 7. The spectrum of **1** in pH 7 aqueous buffer indicates a folded conformation. The minima at ca. 203 and 230 nm lend support to a not-fully-structured $3_{10}$ helix (as in the case of sequences presenting tertiary amides and, hence, were not all H-bonds are possible). The shift to lower wavelengths of the shallower, higher wavelength band by addition of TFE indicates increased $3_{10}$ helix content in this solvent. A right-handed $3_{10}$-helix shows a negative Cotton band centered at ca. 208 nm ($\pi \rightarrow \pi^*$) with a shoulder at ca. 222 nm ($n \rightarrow \pi^*$, $\theta_{222}/\theta_{208}$ ca. 0.3).[45] Thus peptide **1** fulfills our expectation of a partly helical conformation, more structured in the presence of TFE. The situation in the case of the tripodal template is different as our data show that the peptides appear to be already folded even without the addition of TFE as the two negative bands are now centered at 205 and 225 nm. With respect to peptide **1**, the conformation of **2** is shifting, at least in part, from a $3_{10}$ helix toward an α-helix as the 222 nm negative band becomes more pronounced. We have reported that, in polar solvents, conformationally stable, Aib-rich, short peptides shift from a $3_{10}$- to an α-helix.[46] This conformational equilibrium is controlled by the polarity of the solvent

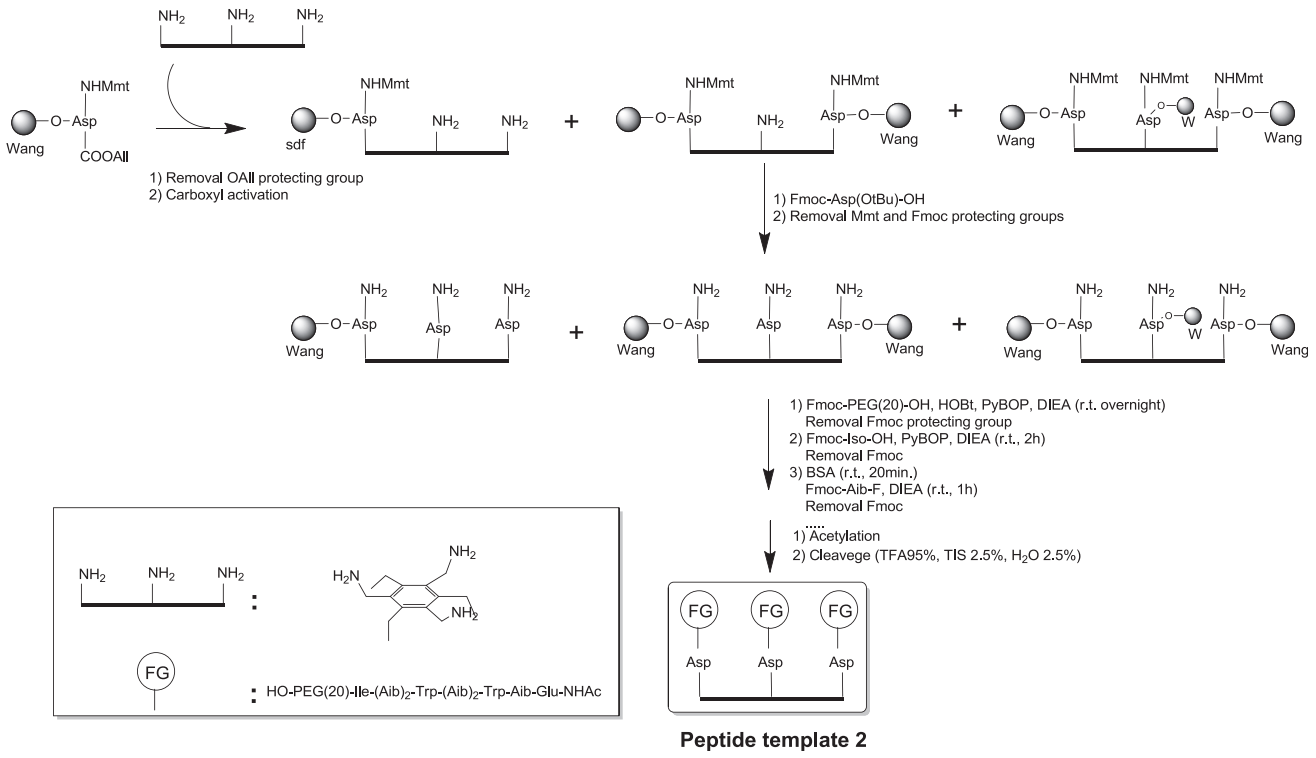


**Fig. 5.** Synthetic strategy followed for the preparation of the tripodal peptide template (**2**).

and it wouldn't be surprising it shifts back to a $3_{10}$ helix in a less polar membrane environment.

The increased helical content may suggest that the three peptides interact reciprocally. Increased helical conformation in templated peptides was first reported several years ago by Mutter in his studies aimed to obtaining template assembled synthetic proteins (TASP).[47] The conformation of the tripodal template appears to be quite robust. The addition of TFE results in a minor shift of the equilibrium toward the $3_{10}$ helix as the $\theta_{222}/\theta_{208}$ ratio slightly decreases in 100% TFE. In view of our hypothesis to obtain an effective HIV-1 fusion inhibitor based on a helical tripodal tris-peptide, this is an important result. The next obvious step is to test the new construct in inhibition studies.

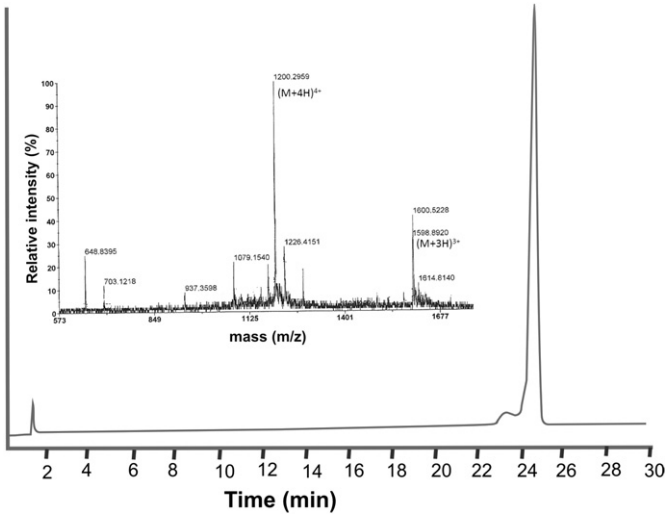


**Fig. 6.** HPLC trace of the peptide template **2** after purification and MS spectrum (inset).

## 2.4. Preliminary inhibition studies

We assessed the ability of peptide **1** and of the tripod conjugate **2** to block viral entry into target cells by evaluating the inhibition of HIV-mediated cell fusion, using a vaccinia virus-based gene reporter system adapted from the procedure developed by Berger and colleagues.[48] Briefly, the assay measures the level of cell to cell fusion between two populations of cells in the presence of viral entry inhibitors. One cell type expresses the viral envelope protein, which is

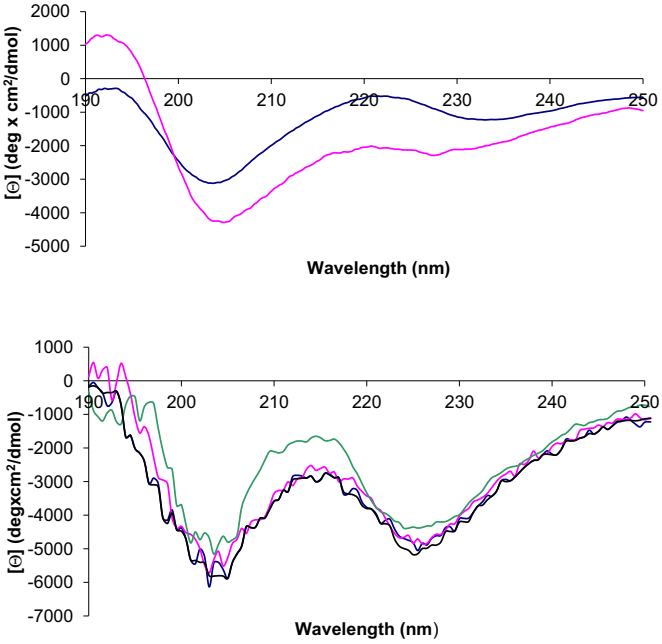


**Fig. 7.** CD spectra of peptide **1**, top, in PBS buffer (pH=7), blue line, and with 25% TFE added, purple line, and tripodal template **2**, bottom, in PBS buffer, black line, with 56% TFE, blue line, 72% TFE, purple line, and 100% TFE, green line.

responsible for binding to the receptor and triggering cell fusion. The other cell type expresses the target receptor, CD4. The cytoplasm of one population also contains bacteriophage T7 RNA polymerase, while the cytoplasm of the other contains a transfected plasmid with the *Escherichia coli lacZ* gene under the control of the T7 promoter. When the two populations are mixed, cell fusion causes mixing of the cytoplasms and consequently activation of the *lacZ* gene in the cytoplasm of the fused cell; the resulting β-galactosidases activity can be measured colorimetrically. Recombinant vaccinia viruses are used as vectors to transfect two populations of NIH 3T3 cells with the exogenous genes described above.

We tested peptide **1** and the tripodal conjugate **2** alongside C14, a peptide that spans 14 residues of the C-ter peptide of gp41 (Table 1). Confirming results from previous tests at the low micromolar range,[18] we found that the C14 peptide has no inhibitory activity up to the concentration of 300 μM; the assay is ideally suited for inhibitors active in the low micromolar range, and therefore we could not explore higher concentrations.[18] Our peptide **1**, which is partly folded in phosphate buffer, displayed no activity in the same range of concentrations. The lack of activity in the range probed by the assay observed for peptide **1** suggests that the sequence is too short to ensure a significant interaction with the target, or that competing peptide oligomerization processes may be involved. It has been show that for C14 peptides, helical content is not necessarily correlated with activity, and in fact over-constraining the peptide may result in loss of activity, possibly because the peptide can be locked in an inactive conformation.[17] Nevertheless, reducing the conformational entropy of the peptide can translate into higher biological activity, even in the absence of strong effects on structure formation.[17,18] In contrast, the tripodal conjugate **2** exhibited inhibitory activity quantified with an $IC_{50}$ of 60±5 μM; this value compares well with the activity of other peptidomimetic agents.[37] While the inhibitory activity is lower than we anticipated, we note that we do observe a strong multivalent effect in the template tripodal peptide. We hypothesize that the tripod stabilizes the helical conformation via controlled oligomerization, while simultaneously allowing enough flexibility for multivalent interactions.

**Table 1**
Cell fusion inhibitory activity observed for peptide **1**, the tripodal conjugate **2**, and C14

| Peptide | $IC_{50}$, μM |
|---|---|
| C14 | ≫300 |
| **1** | ≫300 |
| **2** | 60±5 |

## 3. Conclusions

We have successfully synthesized the peptide sequence AcNH–TEG–Glu-Aib-*Trp*-AibAib-*Trp*-AibAib-*Ile*-Asp–OH (**1**), designed to display the WWI epitope found near the C-terminus of gp41, an envelope glycoprotein decorating the surface of the HIV-1 virus, and have connected it to a tripodal platform based on 2,4,6-triethylbenzene-1,3,5-trimethylamine. Peptide **1** is characterized by a very high helical content with a prevailing $3_{10}$-helix conformation as the consequence of the presence of five Aib in its sequence. The tripodal template **2** is even more structured than **1** thus suggesting a significant interaction between the three sequences connected to the platform. Microwave irradiation proved indispensable for the synthesis of **1** while the synthesis of **2** was better performed step by step following our protocol on solid phase with the critical activation of the carboxylic acids as the fluoride and the use of *N*,*O*-bis(trymethylsilyl)acetamide for the coupling of the amine. Preliminary inhibition assays of HIV-mediated cell fusion indicated that while the single peptide **1** is practically inactive, when it is conjugated to the tripodal platform, it is moderately active. These promising results suggest that our approach constitute a valid alternative to those reported so far. Optimization of the platform to ensure a better match between the tripodal conjugate and its target is currently under investigation in our laboratory.

## 4. Experimental

### 4.1. General

All starting materials, solvents, and resins were obtained from commercial sources and used without further purification. Standard resin loading protocols were used for Wang resin. $^1$H NMR spectra were recorded on a Bruker AC-300 (300.13 MHz) spectrometer operating at 301 K. HPLC chromatograms were recorded using a Shimadzu LC-10AT dual pump system and a Shimadzu SPD-10A UV–Vis detector. HR ESI-mass spectra were obtained using a Perspective Biosystem Mariner spectrometer equipped with a TOF-analyzer.

### 4.2. Synthesis of peptide 1

SPPS of peptide **1** has been performed following standard Fmoc synthesis using 4.5 equiv of each amino acid. Each coupling was repeated twice using in the first run activation by stoichiometric amounts of HATU (2 h), in the second one PyOAP (4.5 equiv 1.5 h, 50 °C). A second more successful protocol employed identical amounts of peptides but MW irradiation (59 W; 75 °C, 5 min) replaced. Only the last amino acid (Fmoc–TEG–OH, 3.5 equiv) without MW irradiation in a single coupling by activating the carboxylic acid with PyAOP/HOBT (3.5 equiv) and letting the mixture to react overnight at rt. After Fmoc removal the mixture was treated with the catalyst (Pd(0)–Tetrakis, 27 mg), $PhSiH_3$ (114 μl) in 1 ml of dichloromethane. After lyophilization a white solid (3.1 mg, 5%) was obtained from the RP-HPLC column. HPLC: (Vydac C4; gradient: $H_2O$/TFA (0.1%)–$CH_3CN$/TFA (0.1%) from 34 to 57% in 60 min, detector UV at 226 nm) 16.5 min (100%). MALDI-TOF $[M+Na]^+$ calculated: 1382.65; experimental: 1381.91.

### 4.3. Synthesis of the peptide template 2

Wang resin (75 mg, 0.0697 mmol) was placed in a small (1.5 ml) reactor and let to swell with MeOH; DCM; DMF in sequence. Fmoc–Asp(OH)–OAll (166 mg, 0.41 mmol) was dissolved in DMF (1 ml) and DIC (56 mg), dichloromethane (0.3 ml), and DMAP (3 mg) were added and the solution let to stir for 2 h. After washing, acetic anhydride (80 μl) and *N*-methylmorfoline (85 μl) in dichloromethane (1 ml) were added. Stirring was continued for 1 h. Fmoc removal was performed with 1 ml of DMF/piperidine (8L2), 15 min. Afterward, Mml (130 mg, 6 equiv), dichloromethane (1 ml), and DMF (0.2 ml) were added and the solution stirred for 2 h. After washing, the catalyst (Pd(0)–Tetrakis, 27 mg), $PhSiH_3$ (114 μl) in 1 ml of dichloromethane were added. After stirring for 2 h under nitrogen, washing was performed first with dichloromethane and DMF and subsequently with 5% DIEA in DCM and with 5% DIEA in DMF. The following reagents and solvents were added to the resin in this order: 0.4 ml of DMF and 80 μl of DIEA, 150 mg of PyBOP in 0.9 ml of dichloromethane and let to stir for 1.5 h and then washed. 1,3,5-Tris-(aminomethyl)-2,4,6-triethylbenzene (23 mg) was dissolved in 1 ml of DMF with 0.3 ml of NMP and 90 μl of DIEA and let to stir for 2 h followed by washing. In the subsequent step 117 mg (0.28 mmol) of Fmoc–Asp(O*t*-Bu)–OH, 150 mg of PyBOP, and 100 μl of DIEA were added, let to stir for 1.5 h followed by washing. After Fmoc deprotection (see above) Mmt was also deprotected

with 1 ml of a solution of acetic acid/trifluoroethanol/dichloromethane (1:2:6), twice for 15 min followed by washing. Fmoc–PEG(20)–OH (123 mg, 3.5 equiv), HOBT (30 mg), PyBOP (115 mg), and DIEA (110 μl) were dissolved in 1 ml of DMF and 0.3 ml of NMP and let to react overnight. After washing Fmoc was deprotected. The coupling was performed with Fmoc–Iso–OH (177 mg, 7.5 equiv), PyBOP (266 mg), DIEA (140 μl) in DMF (1 ml), and NMP (0.3 ml). After Fmoc removal BSA (*N*,*O*-bis(trimethylsilyl) acetamide; 61 μl) in 1 ml of DCM was added and let to stir (15 min, rt) followed by washing with dichloromethane. Fmoc–Aib–F was synthesized dissolving 3.79 mmol (1.2 g) of Fmoc–Aib–OH and Fmoc–Trp(Boc)–OH in 25 ml of DCM and 7.6 mmol (0.61 ml) of iyridine and 7.6 mmol (0.65 ml) of cyanuric fluoride, stirring for 1 h at 0 °C and 2 h at rt. The product was washed in ice water (four times) and dried under $P_2O_5$; with the same procedure Fmoc–Trp(Boc)–F was obtained from Fmoc–Trp(Boc)–OH.

Fmoc–Aib–F (98 mg, 0.3 mmol, 4.3 equiv) dissolved in 1.2 ml of DMF and 75 μl of DIEA were added, let to stir for 15 min. The coupling was then repeated. After washing for 8 min with acetic anhydride (50 μl), and DIEA (55 μl) in dichloromethane Fmoc was removed. The procedure was repeated for all amino acids in the sequence but for the last one (Fmoc–Glu(O*t*-Bu)–OH) that was activated with PyBOP. After Fmoc removal the amine was acetylated. The product was removed from the resin by using 1 ml of TFA 95%. After drying overnight it was dissolved in 1.2 ml of a solution of $CH_3CN$ (40%)–MeOH (40%)–$H_2O$ 19.9%–formic acid 0.1% and sonicated for 30 min. After drying the product was purified on a semipreparative HPLC C4 column gradient $H_2O$/TFA (0.1%)–$CH_3CN$/TFA (0.1%) from 39 to 75% (detector at 280 nm), yield: ca. 10%, Fig. S1. The second HPLC spectra (C4 column gradient $H_2O$/TFA (0.1%)–$CH_3CN$/TFA (0.1%) from 40 to 60%) showed the template **2** after HPLC purification, 99% 24.6 min. ESI-MS: calculated: 4793.5176; found: 4793.676 ($1598.8920\times3\text{-}3H^+$).

### 4.4. Fusogenic activity assay

Anti-HIV activity of peptides **1**, **2**, and C14 (used as control) was assessed using a quantitative vaccinia virus-based HIV-1 fusion.[47] This assay provides a quantitative measure of reporter gene activation in fused cells. HeLa cells (which carry endogenous CXCR4 receptor) were used for both target cell and effector cell populations. Target cells were infected with vCB21R-LacZ (encoding β-galactosidase); effector cells were co-infected with vCB41 (encoding Env from HIV-1 Lav)[49] and vP11T7gene (encoding phage T7 polymerase) at a multiplicity of infection of 10. Following infection for 1.5 h at 37 °C, cells were incubated for 18 h at 32 °C to allow vaccinia virus-mediated expression of recombinant proteins. For inhibition studies of Env-mediated cell fusion, 20 μl of serial dilutions of peptides were added to an appropriate volume of DMEM 2.5% and PBS to yield identical buffer compositions (100 μl), followed by addition of $1\times10^5$ effector cells (in 50 μl media). After 15 min incubation, $1\times10^5$ target cells (in 50 μl media) and soluble CD4 were added to each well. After 2.5 h incubation, β-galactosidase activity of cell lysates was measured upon addition of chlorophenolred-β-D-galactopyranoside (CPRG) using a microplate reader. The inhibitor concentration at which activity was reduced by 50% ($IC_{50}$) was calculated using the appropriate equation in Kaleidograph. Non-commercial reagents were provided through the National Institutes of Health AIDS Research and Reference Reagent Program.

## Acknowledgements

This work was supported in part by NSF Career Award 0449842 to G.G. L.J.P. acknowledges financial support from the ERC (contract UE-239898). We thank the National Institutes of Health AIDS Research and Reference Reagent Program for providing non-commercial reagents. The Padova group gratefully acknowledges the support by MIUR (grant 2006039071) and by the University of Padova (starting grant to L.J.P.).

## Supplementary data

Supplementary data associated with this article can be found in the online version, at doi:10.1016/j.tet.2012.03.078.

## References and notes

1. Chan, D. C.; Kim, P. S. *Cell* **1998**, *93*, 681–684.
2. Zwick, M. B.; Saphire, E. O.; Burton, D. R. *Nat. Med.* **2004**, *10*, 133–134.
3. Markosyan, R. M.; Ma, X.; Cohen, F. S.; Melikyan, G. B. *Virology* **2002**, *302*, 174–184.
4. Gallo, S. A.; Finnegan, C. M.; Viard, M.; Raviv, Y.; Dimitrov, A.; Rawat, S. S.; Puri, A.; Durell, S.; Blumenthal, R. *Biochim. Biophys. Acta-Biomembr.* **2003**, *1614*, 36–50.
5. (a) Melikyan, G. B.; Markosyan, R. M.; Hemmati, H.; Delmedico, M. K.; Lambert, D. M.; Cohen, F. S. *J. Chem. Biol.* **2000**, *151*, 413–423; (b) Malashkevich, V. N.; Chan, D. C.; Chutkowski, C. T.; Kim, P. S. *Proc. Natl. Acad. Sci. U.S.A.* **1998**, *95*, 9134–9139.
6. Skehel, J. J.; Wiley, D. C. *Cell* **1998**, *95*, 871–874.
7. Pöhlmann, S.; Reeves, J. D. *Curr. Pharm. Des.* **2006**, *12*, 1963–1973.
8. Krambovitis, E.; Porichis, F.; Spandidos, D. A. *Acta Pharmacol. Sin.* **2005**, 1165–1173.
9. Steffen, I.; Pöhlmann, S. *Curr. Pharm. Des.* **2010**, *16*, 1143–1158.
10. Valente, S.; Gobbo, M.; Licini, G.; Scarso, A.; Scrimin, P. *Angew. Chem., Int. Ed.* **2001**, *40*, 3899–3904.
11. Harrison, S. C. *Nat. Struct. Mol. Biol.* **2008**, *15*, 690–698.
12. Shepherd, N. E.; Hoang, H. N.; Desai, V. S.; Letouze, E.; Young, P. R.; Fairlie, D. P. *J. Am. Chem. Soc.* **2006**, *128*, 13284–13289.
13. Manfredi, R.; Sabbatani, S. *Curr. Med. Chem.* **2006**, *13*, 2369–2384.
14. Chan, D. C.; Chutkowski, C. T.; Kim, P. S. *Proc. Natl. Acad. Sci. U.S.A.* **1998**, *95*, 15613–15618.
15. Sia, S. K.; Kim, P. S. *Proc. Natl. Acad. Sci. U.S.A.* **2003**, *100*, 9756–9761.
16. Eckert, D. M.; Malashkevich, V. N.; Hong, L. H.; Carr, P. A.; Kim, P. S. *Cell* **1999**, *99*, 103–108.
17. Sia, S. K.; Carr, P. A.; Cochran, A. G.; Malashkevich, V. N.; Kim, P. S. *Proc. Natl. Acad. Sci. U.S.A.* **2002**, *99*, 14664–14669.
18. Wang, D.; Lu, M.; Arora, S. P. *Angew. Chem., Int. Ed.* **2008**, *47*, 1879–1882.
19. Stephens, O. M.; Kim, S.; Welch, B. D.; Hodsdon, M. E.; Kay, M. S.; Schepartz, A. *J. Am. Chem. Soc.* **2005**, *127*, 13126–13127.
20. Horne, W. S.; Johnson, L. M.; Ketas, T. J.; Klasse, P. J.; Lu, M.; Moore, J. P.; Gellman, S. H. *Proc. Natl. Acad. Sci. U.S.A.* **2009**, *106*, 14751–14756.
21. Ernst, J. T.; Kutzki, O.; Debnath, A. K.; Jiang, S.; Lu, H.; Hamilton, A. D. *Angew. Chem., Int. Ed.* **2002**, *41*, 278–281.
22. (a) Welch, B. D.; Francis, J. N.; Redman, J. S.; Paul, S.; Weinstock, M. T.; Reeves, J. D.; Lie, Y. S.; Whitby, F. G.; Eckert, D. M.; Hill, C. P.; Root, M. J.; Kay, M. S. *J. Virol.* **2010**, *84*, 11235–11244; (b) Welch, B. D.; VanDemark, A. P.; Heroux, A.; Hill, C. P.; Kay, M. S. *Proc. Natl. Acad. Sci. U.S.A.* **2007**, *104*, 16828–16833.
23. Ferrer, M.; Kapoor, T. M.; Strassmaier, T.; Weissenhorn, W.; Skehel, J. J.; Oprian, D.; Schreiber, S. L.; Wiley, D. C.; Harrison, S. C. *Nat. Struct. Biol.* **1999**, *6*, 953–960.
24. Weissenhorn, W.; Desson, A.; Harrison, S. C.; Skehel, J. J.; Wiley, D. C. *Nature* **1997**, *387*, 426–430.
25. Chan, D. C.; Fass, D.; Berger, J. M.; Kim, P. S. *Cell* **1997**, *89*, 263–268.
26. Tan, K.; Liu, J. H.; Wang, J. H.; Shen, S.; Lu, M. *Proc. Natl. Acad. Sci. U.S.A.* **1997**, *94*, 12303–12308.
27. Wild, C. T.; Shugars, D. C.; Greenwell, T. A.; McDanal, C. B.; Matthews, T. J. *Proc. Natl. Acad. Sci. U.S.A.* **1994**, *91*, 9770–9774.
28. Kritzer, J. A.; Tirado-Rives, J.; Hart, S. A.; Lear, J. D.; Jorgenson, W. L.; Schepartz, A. *J. Am. Chem. Soc.* **2005**, *127*, 167–178.
29. Toniolo, C.; Benedetti, A. *Macromolecules* **1991**, *24*, 4004–4009.
30. Toniolo, C.; Crisma, M.; Formaggio, F.; Valle, G.; Cavicchioni, G.; Précigoux, G.; Auby, A.; Kamphuis, J. *Biopolymers* **1993**, *33*, 1061–1065.
31. VenkatamaranPrasad, B. V.; Balaram, P. *CRC Crit. Rev. Biochem.* **1984**, *16*, 307–321.
32. Karle, I. L.; Balaram, P. *Biochemistry* **1990**, *29*, 6747–6753.
33. Toniolo, C.; Crisma, M.; Formaggio, F.; Broxterman, Q. B.; Kaptein, B. *Biopolymers* **2004**, *76*, 162–176.
34. Rossi, P.; Felluga, F.; Tecilla, P.; Formaggio, F.; Crisma, M.; Toniolo, C.; Scrimin, P. *J. Am. Chem. Soc.* **1999**, *121*, 6948–6949.
35. Xu, W.; Taylor, J. W. *Chem. Biol. Drug Des.* **2007**, *70*, 319–328.
36. (a) Lu, R. J.; Mader, C. J.; Schneider, S. E.; Tvermoes, N.; Kang, M. C.; Dwyer, J. J.; Wilson, K. L.; Matthews, T. J.; Delmedico, M. K.; Bray, B. *J. Pept. Sci.* **2010**, *16*, 465–472; (b) Eckert, D. M.; Kim, P. S. *Proc. Natl. Acad. Sci. U.S.A.* **2001**, *98*, 11187–11192.
37. Tam, J. P.; Yu, Q. *Org. Lett.* **2002**, *4*, 4167–4170.
38. Ni, J.; Powell, R.; Baskakov, I. V.; DeVico, A.; Lewis, G. K.; Wang, L.-X. *Bioorg. Med. Chem.* **2004**, *12*, 3141–3148.

39. Travisano, P.; Kennan, A. J. *Org. Lett.* **2004**, *6*, 4219–4222.
40. Schnarr, N. A.; Kennan, A. J. *J. Am. Chem. Soc.* **2004**, *126*, 10260–10261.
41. Haynes, S. R.; Hagius, S. D.; Juban, M. M.; Elzer, P. H.; Hammer, R. P. *J. Pept. Res.* **2005**, *66*, 333–347.
42. Pedersen, S.; Jensen, K. *Biopolymers (Pept. Sci.)* **2011**, *96*, 443.
43. (a) Guarise, C.; Prins, L. J.; Scrimin, P. *Tetrahedron* **2006**, *62*, 11670–11674; (b) Guarise, C.; Zaupa, G.; Prins, L. J.; Scrimin, P. *Eur. J. Org. Chem.* **2008**, 3559–3568.
44. Wenschuh, H.; Beyermann, M.; Winter, R.; Bienert, M.; Ionescu, D.; Carpino, L. A. *Tetrahedron Lett.* **1996**, *37*, 5483–5486.
45. (a) Toniolo, C.; Polese, A.; Formaggio, F.; Crisma, M.; Kamphuis, J. *J. Am. Chem. Soc.* **1996**, *118*, 2744–2749; (b) Formaggio, F.; Crisma, C.; Rossi, P.; Scrimin, P.; Kaptein, B.; Broxterman, Q. B.; Kamphuis, J.; Toniolo, C. *Chem.—Eur. J.* **2000**, *6*, 4498–4504.
46. (a) Pengo, P.; Pasquato, L.; Moro, S.; Brigo, A.; Fogolari, F.; Broxterman, Q. B.; Kaptein, B.; Scrimin, P. *Angew. Chem., Int. Ed.* **2003**, *42*, 3388–3392; (b) Bellanda, M.; Mammi, S.; Geremia, S.; Demitri, N.; Randaccio, L.; Broxterman, Q. B.; Kaptein, B.; Pengo, P.; Pasquato, L.; Scrimin, P. *Chem.—Eur. J.* **2007**, *13*, 407–416.
47. Mutter, M.; Dumy, P.; Garrouste, P.; Lehmann, C.; Mathieu, M.; Peggion, C.; Peluso, S.; Razaname, A.; Tuchscherer, G. *Angew. Chem., Int. Ed.* **1996**, *35*, 1482–1485.
48. Nussbaum, O.; Broder, C. C.; Berger, E. A. *J. Virol.* **1994**, *68*, 5411–5422.
49. Broder, C. C.; Berger, E. A. *Proc. Natl. Acad. Sci. U.S.A.* **1995**, *92*, 9004–9008.